New Methodology for Realistic Integration of Sorption Processes Safety Assessments - 14153

U. Noseck*, S. Britz*, J. Flügge*, J. Mönig*, V. Brendler**, and M. Stockmann**
* *GRS Braunschweig, Theodor-Heuss-Str. 4, D-38122 Braunschweig, Germany*
** *Helmholtz-Zentrum Dresden-Rossendorf, P.O.Box 510119, D-01314 Dresden, Germany*

ABSTRACT

Sorption on mineral surfaces of sediments is one important retardation process for radionuclides to be considered in long-term safety assessments for radioactive waste repositories. In the past the K_d-concept with temporally constant values was applied to describe radionuclide retardation in the far field of a repository. This modeling approach has the advantage of being simple and computationally fast but it does not take into account the spatial and temporal changes of geochemical conditions that will occur during the evolution of the repository system, e.g. due to long-term climatic changes. One option to describe the impact of such geochemical changes on radionuclide transport and retardation is the so-called smart K_d-concept. In the present study this new modeling approach is developed allowing the consideration of geochemical changes over time without strongly affecting the computational times of transport calculations. The state-of-the-art transport program r^3t, used for large model areas and very long time scales, was modified to incorporate the smart K_d-concept. The methodology is based on a description of the radionuclide sorption as a function of selected, important environmental parameters (e.g. pH, pCO_2, ionic strength and Ca^{2+}, DIC and the respective radionuclide concentration) using mechanistic sorption models.

First, this approach is developed for a typical sedimentary system covering rock salt and clay formations in Northern Germany. This system mainly consists of tertiary and quaternary sands and clays. However, the approach is applicable to any site of interest. Thermodynamic data were missing for some major minerals present in the model area, such as feldspars and mica, and for relevant elements. To fill these data gaps, an experimental program including batch and column experiments has been conducted. By prior calculations of distribution coefficients for each radionuclide and sediment as functions of the environmental parameters, multidimensional K_d-matrixes are established combining surface complexation and ion exchange. The calculations are performed coupling the geochemical speciation code PHREEQC with the parameter estimation tool UCODE. After implementation of the methodology in r^3t, transport calculations considering long-term changes of geochemical conditions have been performed for selected test cases. The results of the concept applied here are very promising. The concept allows the description of radionuclide sorption and transport through large model areas over very long time frames in dependence of variable geochemical conditions.

INTRODUCTION

A post-closure safety case for a deep geological repository for heat-generating waste requires, amongst other things, a long-term safety assessment [1]. An important aspect in making the safety case is radionuclide transport in geologic formations. In order to assess its consequences over the stipulated assessment period, i.e., one million years for heat-generating waste in Germany [2], numerical models describing flow and transport are applied. Sorption on mineral surfaces is one crucial process retarding radionuclide transport. Its relevance for the calculated end point of the safety assessment, e.g. the potential radiation dose rate in the biosphere, is not yet predictable with sufficient accuracy. On the one hand an increased transport time might cause a decrease in radionuclide concentration by radioactive decay. On the other hand an increased transport time might increase concentrations of dose-relevant daughter nuclides in decay chains. Hence, a description of sorption processes is desirable that is as close to reality as possible.

In recent safety assessment studies, sorption is usually described with temporally and spatially constant distribution coefficients, so-called K_d-values [3, 4, 5]. Since sorption of many radionuclides strongly depends on the geochemical properties of solution and sediments, this approach is justified for steady state hydrogeological and geochemical conditions. However within time frames of one million years, alterations are expected due to environmental variations caused by climatic or geological changes. A straightforward approach to describe changing geochemical conditions is the direct coupling of a transport code with a geochemical code, capable of using thermodynamic sorption models. Such an approach leads to unacceptably long computational times for the large model systems with spatial extensions of several kilometres.

In order to circumvent this problem, a new approach is presented here, in which radionuclide sorption processes in natural systems are treated by the so-called smart K_d-concept. The smart K_d-values are mainly based on mechanistic surface complexation models (SCM) and ion exchange. The values vary in time and space depending on the actual geochemical conditions. The concept developed and introduced here is based on a feasible treatment of the most relevant geochemical parameters in the transport code as well as on a matrix of smart K_d-values pre-calculated in dependence on these parameters. Sorption is described by a so-called component-additivity approach (bottom-up strategy), i.e. sorption for each element on a particular geological unit (a mixture of a number of minerals) is described as the sum of the sorption of the element on every single mineral fraction [6,7]. In the first stage this approach is developed for a typical sedimentary system covering rock salt and clay formations in Northern Germany.

The approach necessitates a comprehensive thermodynamic database including data for surface complexation and ion exchange for the mineral phases and elements (radionuclides) considered in the safety assessment calculations. By defining the most relevant mineral phases occurring in the sedimentary systems in Northern Germany and by reviewing existing sorption data, especially the Rossendorf Expert System for Surface and Sorption Thermodynamics (RES^3T database) [8], most crucial data gaps have been identified. Specific batch sorption experiments have been planned and performed to generate lacking data and to test the component-additivity approach.

The databases and the procedure to create a matrix of smart K_d-values is described in detail in [9]. The newly developed approach, the experimental program to determine missing thermodynamic sorption data, and the application of the approach to two-dimensional transport models are presented here.

DESCRIPTION

Concept

In the first step the concept is developed for a typical sedimentary system in Northern Germany as described by the comprehensive data set for the Gorleben site. The model used here is based on a schematic cross section through the Gorleben area, which summarizes all main geological and hydrogeological characteristics of the site under present conditions (Fig. 1) [10]. It comprises three geological units, representing the lower aquifer, the aquitard, and the upper aquifer. The lower aquifer is characterized by high salt concentrations in the groundwater, resulting from the contact of the lower aquifer to the cap rock of the salt dome and leaching of salt, while the upper aquifer is characterized by low salt concentrations.

Groundwater recharge takes place at the surface. Part of this water is drained to the lowlands of the river Elbe, while the other part may infiltrate through hydraulic windows of the aquitard down to the lower aquifer. At the area of contact between the salt dome and lower aquifer, salt can be dissolved increasing the salt concentration and the density of the groundwater. From the contact with the salt dome, the water flows to the north and sinks down in the so-called northwestern rim syncline. Apart from that, the water

can rise up into the upper aquifer through the hydraulic windows or through the aquitard, resulting in locally elevated layers of salt water underlain by less saline water and in salt water occurrences at the surface.

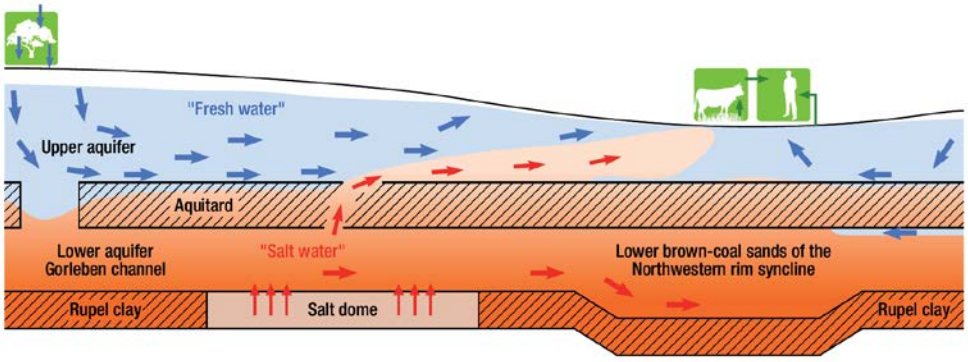

Fig. 1. Schematic north-south striking cross section of the hydrogeological system at the Gorleben reference site, modified from [10], lateral extension app. 16 km, horizontal extension up to 480 m.

The cross section shown in Fig. 1 is the basis for the development of the new modeling concept for considering radionuclide sorption processes in safety assessments. A key feature of the concept is the description of sorption by the component additivity approach [9], in which the contribution of the sorption of one element is considered on every single mineral fraction of the respective geological unit. Therefore, for each geological unit the composition for each of the most relevant mineral phases is compiled [11]. Relevant mineral phases in the Gorleben system are quartz, feldspar, mica, gibbsite, goethite, illite and kaolinite. More details including the exact composition of each geological unit can be found in [11].

The elements (radionuclides) to be considered have been identified based on (i) their relevance for long-term safety, (ii) the propensity to sorb, and (iii) the availability of comprehensive and reliable thermodynamic data. As a result Ni, Se, Cs, Cm, Am, Pu, U, Th, Np, and Ra have been selected for the calculations. In this paper, exemplary results for Cs are shown. In order to describe the sorption processes by a geochemical speciation code, the thermodynamic data for the elements and mineral phases were extensively reviewed. Since for some of the relevant mineral phases, particularly feldspars and mica, hardly any sorption parameters for surface complexation models were available, appropriate sorption experiments with cesium (Cs), strontium (Sr), and europium (Eu, as a homologue for Cm and Am) on orthoclase and muscovite needed to be performed.

For the chosen approach, environmental parameters, which affect sorption of these elements, have to be selected. In the first step a limited number of parameters were identified: pH-value, ionic strength, concentrations of calcium [Ca] and dissolved inorganic carbon [DIC], and the concentration of the radionuclide itself. Sensitivity analyses confirm that usually only two or three parameters strongly contribute to the variation of the sorption coefficient in the selected parameter range. The transport and specific treatment of the environmental parameters have been implemented into the transport code r^3t [12] as briefly described below. In addition the most important complexing and competing ions (silicon, aluminum and iron) have been considered indirectly for calculating the multidimensional matrix of smart K_d-values (see below) by assuming that the concentrations of the ions SiO_3^{2-}, Al^{3+}, and Fe^{3+} are primarily determined by equilibria with solubility limiting mineral phases (quartz, gibbsite and hematite, respectively).

One feature of the new approach is that all smart K_d-values are pre-calculated by the geochemical code PHREEQC [13] for the defined range of environmental parameters and are stored in a multidimensional matrix [9, 11]. As an example a part of the multidimensional matrix, i.e. the dependence of the smart K_d-value from pH, ionic strength and Cs-concentration is shown in Fig. 2 for Cs and Am. It is clearly visible that sorption of Cs is only affected by pH, whereas for Am the impact of DIC concentration and ionic strength (although less so) also play a role. The transport code r^3t selects the appropriate value from this matrix for the specific environmental parameter values calculated at each time step and spatial point of the model area.

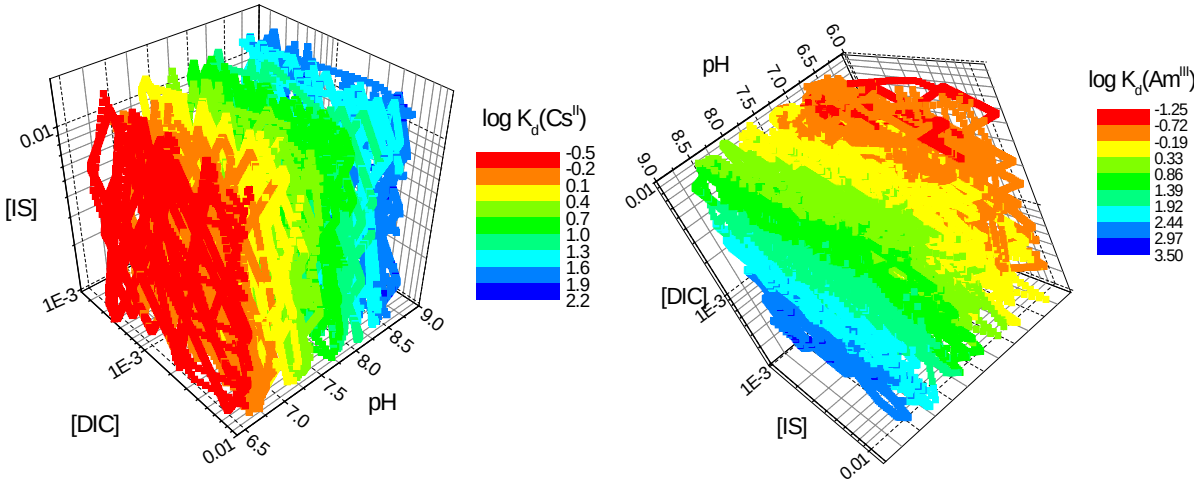

Fig. 2. Multidimensional K_d-matrix for Cs^+ (left) and Am^{3+} (right) as a function of pH, ionic strength IS, and [DIC] (K_d in $m^3\ kg^{-1}$, logarithmic scale).

A crucial aspect concerning the implementation of the environmental factors into the transport code is that the pH-value is affected not only by proton transport but also by chemical reactions with the dissolved ions (preferably DIC and Ca) and mineral phases of the sediments. According to the results from site investigation, the main reactions in the Gorleben aquifers are calcite dissolution (mainly in the upper aquifer), microbial degradation of sedimentary organic carbon (SOC) causing enhanced CO_2 partial pressures (DIC source), and dissolution of feldspars [14]. At present, dissolution and precipitation of calcite are considered as the most relevant reactions affecting the pH-value: the pH is increased by calcite dissolution and decreased by calcite precipitation.

The major features of the treatment of the environmental factors in the transport code can be summarized as follows: In the first time step, the Ca and DIC concentrations as well as the pH-value are calculated on the basis of the transport calculation and possible sources (e.g. microbial DIC formation). On this basis it is examined, whether the solution is under- or oversaturated with respect to calcite. At this stage it is assumed that there will be always enough calcite in the system. Calcite will be precipitated if oversaturated and calcite will be dissolved if undersaturated. The amount of precipitated or dissolved calcite and the resulting concentrations for Ca and DIC as well as the new pH-value are then iteratively calculated based on thermodynamic considerations. The new equilibrium concentrations together with the current radionuclide concentration calculated in the time step is used to select the K_d-value from the multidimensional matrix for each radionuclide for this time step. Finally proton and hydroxyl ion concentrations, which are used for the next time step, are calculated from the equilibrium pH-value. All equations employed for the determination of the saturation index of calcite and for the calculation of the equilibrium conditions as well as all the details of the concepts are documented in [11].

Experimental Program

For some of the relevant mineral phases, particularly feldspars and mica, hardly any sorption parameters for surface complexation models are available in the literature (Tab. I). These findings are based on the RES^{3}T data base of the Helmholtz-Zentrum Dresden-Rossendorf serving as a state-of-the-art thermodynamic data base [8]. Hence, batch sorption experiments have been performed with long-term safety relevant mono-, bi-, and trivalent cations, such as Cs^+, Sr^{2+}, and Eu^{3+} in combination with orthoclase and muscovite which are representative minerals for many sites in Northern Germany.

TABLE I. Number of SCM data sets retrieved from RES³T

Mineral/ Mineral group [a]	Quartz	Feldspars	Mica	Fe(III)-oxide/-hydroxides	Aluminum-hydroxides	Kaolinite	Mixed-layer clay minerals	Σ minerals
Radionuclides								
Cs^+, (Rb^+)	12	1[b]	[b]	7	2		5	27
Ra^{2+}, (Sr^{2+}, Ba^{2+})	7	[b]	[b]	20		7	5	39
Ni^{2+}	9			6	2	5	22	44
Am^{3+}, Cm^{3+}, (REE)	19	[b]	[b]	40		9	65	133
Pu^{4+}, Th^{4+}, (Ce^{4+}, Np^{4+}, U^{4+})	8	[b]	[b]	40		4	13	65
NpO_2^+	3		6	18	11	2	6	46
UO_2^{2+}	64	2	5	196	7	15	25	314
SeO_4^{2-}				15	1			16

[a] applicable for site-relevant minerals (including amorphous Silica and $Al(OH)_3$)
[b] additional SCM-data from batch experiments GRS
( ) Analogues, i.e. elements with similar electronic structure and chemical properties

Objectives of the conducted batch experiments include the assessment, evaluation as well as processing of the collected sorption data by means of the geochemical speciation code PHREEQC in combination with UCODE. It is also aimed at verifying the chosen component additivity approach referring to the description of sorption behavior of natural or synthetic sediments by means of its constituents. Further information regarding the applied minerals may be obtained from [15].

Experimental set-up

First, titration experiments are conducted to get an insight into protonation and deprotonation characteristics of the applied minerals. Following the experimental set-up of [6], suspensions of muscovite and orthoclase in 0.1 mol $(dm)^{-3}$ sodium perchlorate ($NaClO_4$) are applied to conduct titration experiments in order to derive protolysis constants via computational evaluation of the data sets. Mineral samples are treated separately under argon atmosphere. 0.01 mol $(dm)^{-3}$ HCl and 0.001 mol $(dm)^{-3}$ NaOH solutions are applied for the continuous titration of 80 $(cm)^{-3}$ of 0.1 mol $(dm)^{-3}$ $NaClO_4$ and 1 g suspended solid phase. Titration starts after the background solution (0.1 M $NaClO_4$) is equilibrated with the mineral which takes approximately 4 months. The titration-program consists of an acid and accordingly base application of 60 – 2000 $(cm)^{-3}$ every 2 minutes. Obtained results correspond to expectations.

For batch-experiments the minerals are sieved to 63 – 200 µm. Two solid-liquid ratios (M/V) of 1/20 and 1/80 are applied in 0.01 mol $(dm)^{-3}$ $NaClO_4$, each M/V covering an element concentration of 10^{-5}, 10^{-6}, 10^{-7}, and 10^{-8} mol $(dm)^{-3}$. By adding appropriate amounts of 0.01 mol $(dm)^{-3}$ - 1 mol $(dm)^{-3}$ HCl and NaOH to the suspensions, pH values ranging between 7 and 9 are established over a time range of approximately three months. Measurements are performed in triplicate with subsequent statistical analysis. Throughout the whole experiment, samples are shaken head first. After the suspensions show no significant pH variations over 24 hours, Eu is added in various concentrations (ICP-MS CertiPUR norm-solution, 1 g $(dm)^{-3}$ Merck KGaA, 64271 Darmstadt, Germany) and equilibration between the element and the suspension is assumed to take place within 24 hours.

Geochemical Modeling

PHREEQC is a geochemical modeling code for simulating chemical reactions and transport processes in water, including speciation and batch-reaction, 1D reactive transport, and inverse modeling. For speciation and batch-reaction calculations, PHREEQC numerically solves sets of nonlinear mole-balance and mass-action equations. UCODE is a universal parameter estimation code that can be used with existing process models (software packages) to perform sensitivity analysis, data needs assessment, calibration, prediction, and uncertainty analysis [16]. Data exchange between UCODE and PHREEQC is managed via text input files and text output files. Furthermore, the required models have to be executed from a single batch file, and simulated values need to be continuous functions of the parameter values [16]. Fig. 3 illustrates the coupling of PHREEQC with the version UCODE_2005 as used in this study.

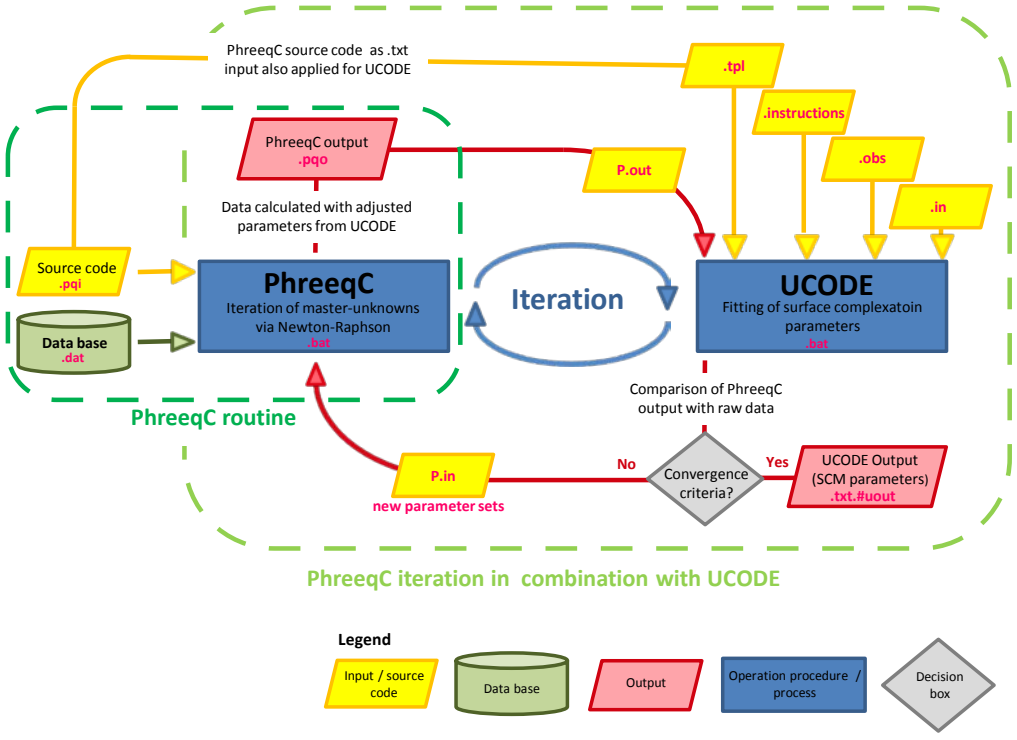

Fig. 3. Scheme of the coupled geochemical speciation code PHREEQC with UCODE_2005 as applied in this study [15].

The surface complexation models (SCM) are developed in a stepwise approach. Firstly, input files are written for the geochemical speciation code PHREEQC in order to iteratively determine surface site area (SSA), surface site density (SSD), and protolysis constants (pK-values) of each mineral, respectively, by

fitting experimental titration data. This fitting is accomplished by coupling PHREEQC with the parameter estimation code UCODE_2005 (Fig. 3). The following step comprises further development of the PHREEQC input file by means of program code adaptation to obtain stability constants of surface complexation and exchange reactions. These advanced files represent the surface complexation models of muscovite and orthoclase. Within these final SCM, the determined SSA, SSD, and protolysis constants pK1 and pK2 are treated as fixed values, whereas stability constants are iteratively determined using UCODE_2005. For detailed information concerning the program code, see [15].

Comparing measured data sets with simulations based on the determined surface complexation parameters (SCP) offers an instrument to evaluate their robustness on the one hand, but also holds the opportunity to verify the component additivity approach applied in this study on the other hand. Furthermore, experimental results from another experimental and modeling study published in [17] have been selected to qualify the developed models as well as the component-additivity approach. These are experimental data from batch experiments with uranium on natural and synthetic sands performed by Helmholtz-Zentrum Dresden-Rossendorf [18].

Transport Modeling

A two-dimensional model for testing the new approach was set up based on the schematic cross section (Fig. 1) and the geological and hydrogeological information given by numerous publications for the Gorleben site [10, 14]. The length of the area of interest is 16.4 km and it has a maximum depth of 400 m (Fig. 4). Three different units represent a lower and an upper aquifer (both 100 m thick) with an intercalated aquitard (50 m thick). The northwestern rim syncline is realized in the model with an additional thickness of the lower aquifer of 150 m. The aquitard is locally interrupted by two hydraulic windows; one with a width of 500 m close to the southern boundary of the model and a second one at the northern boundary of the northwestern rim syncline. The contact of the lower aquifer to the cap rock of the Gorleben salt dome is marked in red in Fig. 4. All figures of the model and simulation results are exaggerated by a factor of 10 in this paper.

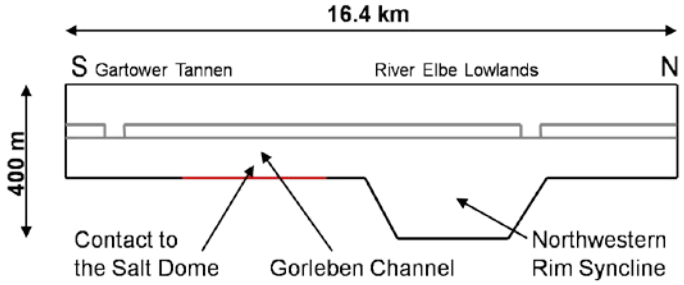

Fig. 4. Geometry of the groundwater flow and transport model

Values for the hydraulic parameters are taken from different publications about the Gorleben aquifer system (cited in [19]). The permeability k is $1 \cdot 10^{-12}$ m^2 for the aquifers and $1 \cdot 10^{-16}$ m^2 for the aquitard. The porosity φ is 0.2 (aquifers) and 0.05 (aquitard). A uniform longitudinal dispersion length α_L of 10 m, a transversal dispersion length α_T of 1 m, and a molecular diffusion coefficient D_m of $1 \cdot 10^{-9}$ m^2 s^{-1} are set for the entire model domain. The hydrogeological flow field is calculated with the code d^{3}f (distributed, density-driven flow), which is able to calculate density-driven groundwater flow [20]. The salt concentration c_{rel} is given as relative concentration in a range between 0 (containing no solutes) and 1 which corresponds to a saturated NaCl brine (360.54 g (dm)$^{-3}$ at 20°C). Depending on these values, the program r^{3}t calculates the ionic strength [11].

In a first step, the present flow field is modeled, which developed since the end of the Weichselian cold stage and the beginning of the Holocene 11,500 a ago. After 11,500 a model time, the results for the flow field and the salt distribution are compared to the present state. Initial conditions for the salt concentration are set according to the salt distribution at the beginning of the Holocene. The lower aquifer and the aquitard show saline conditions, while in the lower part of the upper aquifer, there is a transition zone of 30 m to fresh water conditions in the upper part of the aquifer. Present state boundary conditions are applied. In order to be able to compare the simulation results using the smart K_d-concept to those employing conventional K_d-values, the flow field and salt concentration should not be too complex. Thus, constant climatic conditions with constant boundary conditions were assumed and results are evaluated at a model time of 160,000 a.

Boundary conditions are taken from different publications [10, 14]. In the Gorleben Channel, where the lower aquifer has contact to the salt dome, salt can be dissolved. Therefore, the salt concentration at this model boundary is set to $c_{rel} = 1$ at a length of 4 km. At the southern and northern part of the model surface, groundwater recharge of 160 mm a^{-1} is defined as inflow of freshwater with a velocity of $5.1 \cdot 10^{-9}$ m s^{-1} and a salt concentration of $c_{rel} = 0$. In the center of the surface, a hydrostatic pressure is given. Here, fresh water may infiltrate ($c_{rel} = 0$) or groundwater of different salinity may be discharged (in- and outflow boundary condition). At the northern boundary, an inflow of fresh groundwater into the lower aquifer is defined with a velocity of $6.3 \cdot 10^{-8}$ m s^{-1} and a salt concentration of $c_{rel} = 0$. For details see [19].

For transport simulations, the environmental parameters have to be quantified for the initial and boundary conditions. Based on the groundwater chemical data for the Gorleben area, the parameters pH, Ca, and DIC have been derived (Tab. II). Based on the environmental parameters and the concentrations of the respective radionuclides, calculated for each point in time and space, the code r^3t selects the appropriate smart K_d-value from the multidimensional K_d-matrix. At this stage the assignment of smart K_d-values is only applied to the aquitard and the upper aquifer. For the lower aquifer – where a Pitzer formalism would be more appropriate to account for the ion-ion-interactions in highly saline groundwater – conventional K_d-values are set.

TABLE II. Precipitation and initial groundwater composition according to [21]

Parameter	Unit	Upper Aquifer	Aquitard	Lower Aquifer	Precipitation water
pH	[-]	7.5	8.0	7.2	5.6
Ca	[mol m^3]	1.21	0.24	22.28	0.025
DIC	[mol m^3]	2.70	3.57	4.75	0.002

For the transport calculations, a Dirichlet condition is set for the inflow into the lower aquifer. The chemical composition of the inflowing groundwater is assumed to be identical to the formation water of the lower aquifer (Tab. II). An in- and outflow boundary condition is stated for the model surface, depending on the flow direction. The chemical composition of the outflowing water at the surface equals the calculated actual chemical composition of the groundwater. In case of an inflow, the chemical composition is defined equal to a typical composition of precipitating water (Tab. II). The mineral composition of the hydrogeological units is accounted for during the pre-calculation of the multidimensional smart K_d-matrix and does not have to be specified in the r^3t calculations [11].

DISCUSSION

Geochemical Modeling

Fit and evaluation of titration data

Fig. 5 (left) compares the measured and fitted data sets regarding muscovite and orthoclase titration curves. Major characteristics of both graphs are well reproduced even though small differences between the measured and the fitted data sets are apparent. Correlation coefficients of R = 0.944 for muscovite and R = 0.992 for orthoclase imply a high quality of fit. The curve of the orthoclase data set shows only small offsets, while muscovite is represented perfectly except for slight differences relating to higher pH-values. The fit results are summarized in Tab. III. In most cases the parameters fall well within the range of literature values. An exception is the rather high SSD value for orthoclase. However, one has to consider the specific mineral treatment by the vendor. For details see [15].

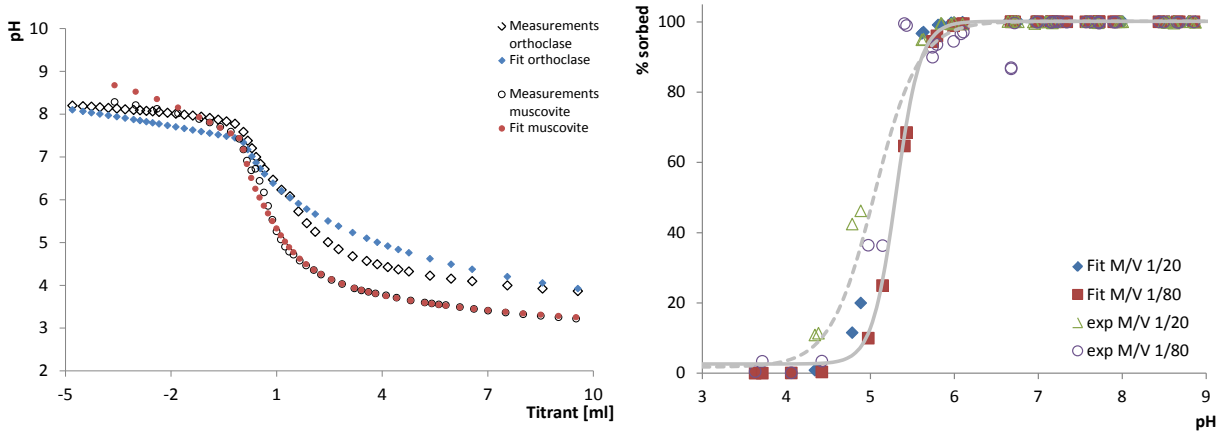

Fig. 5. Left: Comparison between the fitted and experimental titration data for muscovite (circles) and orthoclase (diamonds). Right: Sorption edge of Eu^{3+} on orthoclase as a function of pH for two M/V ratios. Regressions illustrate sorption edges of experimental (dotted line) and fitted batch data sets (solid line).

TABLE III. Mineral-specific SCP obtained from titration-curve fits for muscovite and orthoclase.

Surface complexation parameter	Muscovite	Orthoclase
SSA [m^2g^{-1}]	5.96	15.2
SSD [sites nm^{-2}]	1.73	7.18
pK1	8.04	8.04
pK2	-6.7	-6.8
R	0.944	0.992

Fit and evaluation of batch sorption experiments

The derivation of surface complexation constants for Cs^+, Sr^{2+}, and Eu^{3+} follows the scheme outlined in Fig. 3. The parameters given in Tab. III are fixed for the whole iteration process. Orthoclase, as a rather uniformly structured feldspar, employs only one sorption site (a). In contrast muscovite, as a mica with a sheet structure, is described by strong (a) and weak sorption sites (b). In addition, muscovite also provides cation exchange sites. The initial loading of these sites is zero for all three cations. For both minerals, monodentate complexes are applied in all fits. Tests with more complex sorption reactions, e.g. bidentate complexes, failed to yield a better goodness of fit. Exemplarily, Fig. 5 (right) shows experimental and

fitted data of Eu^{3+} sorbed on orthoclase. Similar good fits are achieved for Eu^{3+} on muscovite, where the mineral's cation exchange is evident and satisfactorily modeled. Tab. IV summarizes the derived SCP for Cs^{+}, Sr^{2+}, and Eu^{3+} sorption on muscovite and orthoclase. Thus, the overall data set comprises SSD, SSA, and pK-values (see Tab. III), as well as stability constants for the surface complexes Log_K and and logK_EX for the cation exchange (see Tab. IV).

The thermodynamic sorption data derived above were used to test the validity of the proposed component additivity approach. Therefore, synthetic sediments have been defined and respective experiments were performed. The synthetic sediment is composed of 10 wt% orthoclase, 10 wt% muscovite and 80 wt% quartz, similar to the sedimentary composition of the upper aquifer at the Gorleben site, Northern Germany. Experiments are conducted with Eu^{3+} for three pH-values ranging between 3 and 8, two different M/V ratios (1/80 and 1/320 g $(dm)^{-3}$) and using three different Eu^{3+} concentrations (10^{-5}, $5 \cdot 10^{-6}$ and 10^{-6} mol $(dm)^{-3}$). In addition to the data sets for muscovite and orthoclase given in Tab. III and Tab. IV, a set of SCP for quartz is taken from literature [22].

TABLE IV. Mineral-specific surface complexation and ion exchange constants, and goodness of fit (R).

Surface complexation parameter	**Muscovite**			**Orthoclase**	
	Cs^{+}	Sr^{2+}	Eu^{3+}	Sr^{2+}	Eu^{3+}
logK a	1.12	-4.1	3.5	-4.8	1.95
logK b	-5.66	-6.6	1.6		
logK_EX	-1.23	-0.9	-0.6		
R	0.9512	0.8558	[a]	0.9123	[a]

[a] Eu^{3+} fits are obtained by manually adapting fitted to experimental data. Hence, no correlation coefficient is obtained.

Description of sorption of synthetic sediments using a component additivity approach

Fig. 6 shows the experimental sorption curves for the synthetic sediment as well as the prediction based on the component additivity approach. Obviously there is a satisfying correlation of measured and modeled data regarding all sorption trends without limitations for all ranges of element concentrations. The good prediction of the experimental data of the synthetic sediment demonstrates the validity of the chosen component additivity approach. Secondly, the prediction also provides strong support of the assessed Eu^{3+} SCP regarding both minerals.

Supplementary experimental results have been selected to further qualify the component additivity approach for another element. Experimental data from sorption batch experiments with uranium on natural and synthetic sands performed by HZDR published in [17] have been used. Protolysis constants and log K-values for simulating sorption reactions of uranium on quartz, muscovite and iron oxide (goethite) data sets are taken from the RES³T data base. For the specific surface area, the values given in [17] are applied. The synthetic sand consists of 95 % quartz and 5 % muscovite, itself containing 6 % iron oxide. Data for iron oxide is substituted by goethite data which provides a good agreement between the experimental and simulated curve (Fig. 7). These results increase confidence in the models and the approach used. Additional calculations with natural sand including the dependence on the initial uranium concentration show similar satisfying results.

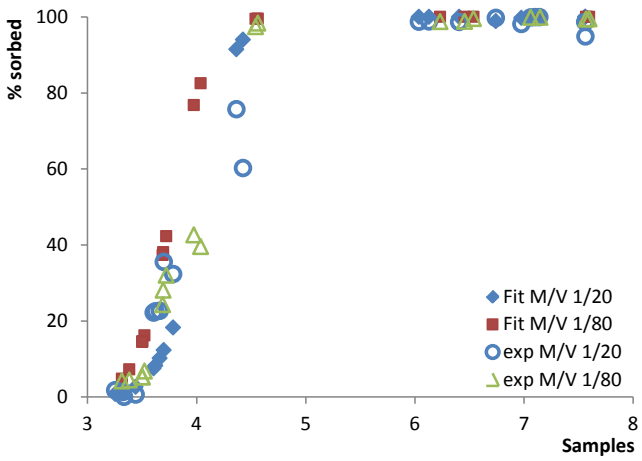

Fig. 6. Sorption curves of the synthetic sediment: experimental data (open symbols), fitted data set (full characters). Good correlation between both data sets support the chosen bottom-up approach.

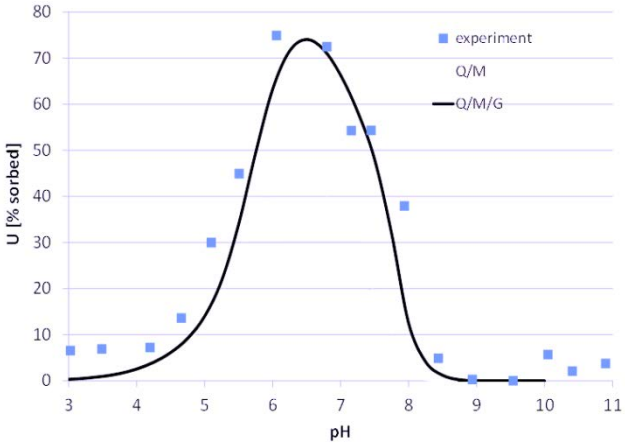

Fig. 7. U(VI) sorption on synthetic sand. Experimental data [17] compared to simulation results for a mixture quartz, muscovite and goethite (Q/M/G).

Transport Modeling

The results of the transient flow simulations including distribution of the salt concentration after 160,000 a model time are discussed and illustrated in Fig. 8. The model shows a clear decrease in salt concentrations after 160,000 a particularly in the lower aquifer and the northwestern rim syncline. Salt concentrations of $c_{rel} = 1.0$ only remain at the interface with the salt dome, where salt is constantly dissolved. In the northwestern rim syncline, the salt concentration is reduced to about $c_{rel} = 0.4 – 0.6$. This reduction results from the inflow of fresh water into the lower aquifer which dilutes the salt water in the rim syncline and transports it up to the surface. The areas of groundwater discharge at the surface are broadened. General flow directions are preserved. The flow velocity is slightly reduced, especially in the upper aquifer. After 160,000 a model time, the salt concentration and the groundwater flow almost meet steady-state conditions. The dominant process for the transport of the salt is advection due to relatively high flow velocities.

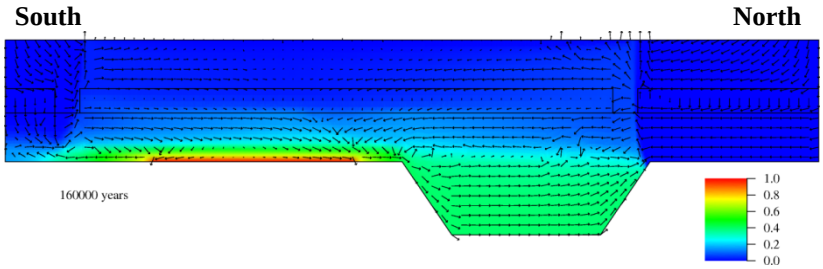

Fig. 8. Relative salt concentration and velocity field for constant boundary conditions at 160,000 a model time; length of velocity vectors proportional to velocity.

On the basis of the transient flow fields, transport calculations with code r^{3}t and the newly implemented approach are performed. In Fig. 9 the conditions for the environmental parameters are shown for the initial state of the model calculation and at a model time of 160,000 a. After 160,000 a model time, the distribution of the environmental parameters has changed according to the flow field, the boundary conditions and the geochemical interactions of the environmental parameters.

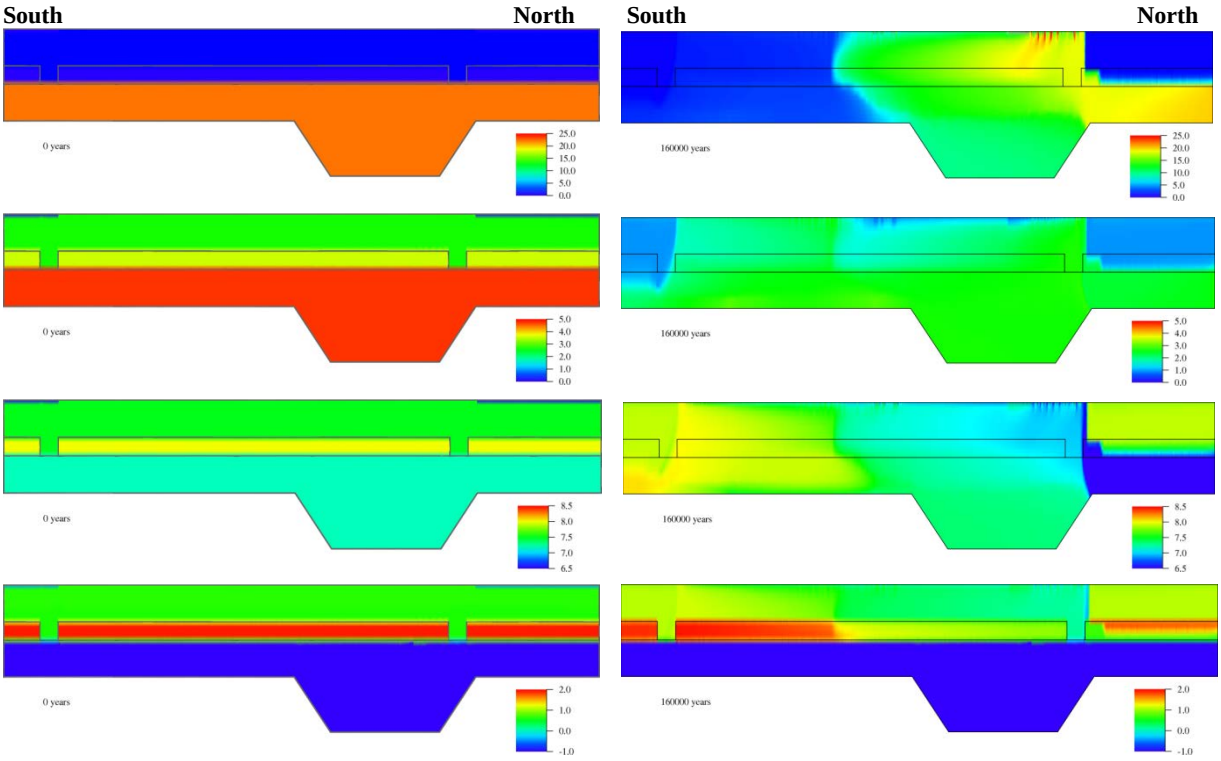

Fig. 9. Distribution of environmental parameters at the beginning of the model calculation (left) and after 160,000 a model time (right) for [Ca] (mol m^3, top), [DIC] (mol m^3, 2nd line), pH (without unit, 3rd line) and corresponding smart K_d-values for Cs (m^3 kg^{-1}, bottom).

In the northern and southern part of the upper aquifer, groundwater recharge takes place. The rainwater has a low pH-value of 5.6, while the formation water in the upper aquifer has an initial pH-value of 7.5. Additionally, the rainwater has low contents of [Ca] = 0.025 mol m^{-3} and [DIC] = 0.002 mol m^{-3} compared to the initial Ca and DIC concentrations in the upper aquifer of [Ca] = 1.21 mol m^{-3} and

[DIC] = 2.70 mol m^{-3}. Due to the influence of the modestly mineralized rainwater, the Ca and DIC concentrations in the recharge areas decrease compared to the formation water of the upper aquifer. As a consequence of the low concentrations of Ca and DIC, calcite dissolves causing an increase of the pH-value compared to the initial value of the formation water. In the center of the upper aquifer, the groundwater is still affected by the groundwater recharge in the south and in the north. Calcite is dissolved, the pH-value increases, and the Ca and DIC concentrations are decreased.

The aquitard has a low permeability, and therefore low flow velocities are to be observed here. Changes of the environmental parameters in the aquitard are mainly caused by diffusion from the lower and the upper aquifer into the aquitard. As a consequence, trends of the changes in the two aquifers can be traced into the aquitard. The lower aquifer shows different zones of the geochemical environment: The region of formation water inflow north of the northwestern rim syncline, the region of influence of the hydraulic windows with complex groundwater flow, and the region with the high salinities at the contact to the salt dome and in the northwestern rim syncline. Initially, the formation water is not in equilibrium with calcite. Initial environmental parameters were defined according to [14] without equilibrating them prior to the simulations. Therefore, calcite precipitates in the lower aquifer. After 160,000 a, this effect is most evident in the northern part of the lower aquifer, where formation water is entering the model area. As a consequence, the pH-value as well as the Ca and DIC concentrations of the inflowing formation water are decreasing after entering the model area.

In the vicinity of the northern hydraulic window, part of the groundwater flow from the lower aquifer is directed through the hydraulic window to the upper aquifer and from there to the south. At the same time, part of the groundwater from the upper aquifer descends through the hydraulic window, mixes with the groundwater from the lower aquifer and is then directed to the south. Thus in the lower aquifer, the alteration of the geochemical parameters can be traced from the northern part, where the groundwater inflow takes place, to the upper parts of the lower aquifer south of the northern hydraulic window. The complex flow patterns additionally result in a plume with higher Ca and DIC concentrations in the upper aquifer south of the hydraulic window. In this region, the pH-value is lower than given by the initial conditions and it is also lower than in others parts of the upper aquifer.

The area in the vicinity of the interface with the salt dome and the northwestern rim syncline is characterized by a high salinity, i.e. a high ionic strength. It is important to note that the smart K_d-concept is so far not designed for dealing with very high ionic strengths as featured by saturated brines. Therefore, calculated environmental parameter values in this area have to be handled with care, since at this stage the Pitzer formalism is not implemented in the concept. Ca and DIC concentrations decrease compared to the initial conditions as a result of the inflow of recharging rainwater, which mainly enters the lower aquifer through the southern hydraulic window. Relatively high DIC concentrations remain in the lower parts of the lower aquifer. At the same time, the mentioned region shows a considerable decrease of the pH-value.

The smart K_d-value of Cs-135 after the first time step is calculated to be 84.6 $m^3\ kg^{-1}$ in the aquitard. In the upper aquifer, the smart K_d-value is 4.4 $m^3\ kg^{-1}$ for the lower part and 4.8 $m^3\ kg^{-1}$ for the upper part of the aquifer. After 160,000 a model time the smart K_d-value very well reflects the evolution of the environmental parameters, in the upper aquifer as well as in the aquitard. Since the pH-value is the most important parameter, the smart K_d-value is higher in areas with higher pH and vice versa. Additionally the higher content of clay minerals causes the higher smart K_d-values in the aquitard. The smart K_d-value in the aquitard decreases, especially above the northwestern rim syncline, where the pH-value is lowest. Where groundwater from the lower aquifer rises to the upper aquifer and is transported to the south, lowest smart K_d-values of $1 – 2\ m^3\ kg^{-1}$ in the upper aquifer are found. Elevated smart K_d-values of approx. 12 $m^3\ kg^{-1}$ can be observed in the groundwater recharge areas. High smart K_d-values of up to approx. 14 $m^3\ kg^{-1}$ are found in the vicinity of the southern hydraulic window according to the highest pH-values found there.

On that basis the transport of Cs-135 is calculated, assuming a stylized inflow as point source with a constant flux of $4.35 \cdot 10^{-11}$ mol s^{-1} in a time frame between 12,500 and 111,500 a [11]. The distribution of Cs-135 after 160,000 years model time is shown in Fig. 10. After upward and northward transport through the lower aquifer, the aquitard is reached. Due to high smart K_d-values and mainly diffusive transport in this unit, Cs-135 has only entered about one third of the aquitard thickness. This observation is plausible. However, it is necessary to apply longer model times considering climatically driven changes to enable a deeper insight into the radionuclide transport through the aquitard and the upper aquifer. Such simulations will be performed in the near future.

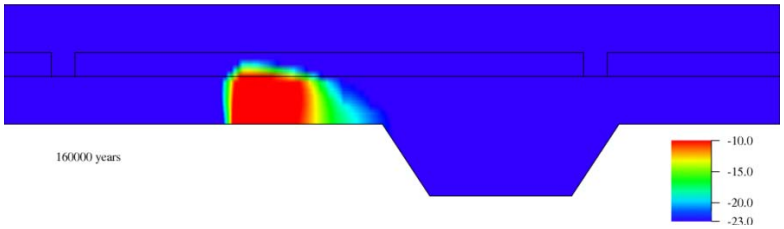

Fig. 10. Distribution of Cs-135 after 160,000 a, logarithmic scale [mol m^{-3}].

Summarizing the calculations shown here for a model time of 160,000 a with constant boundary conditions, the transport of the radionuclides is dominated by advection. The environmental parameters reflect well the interaction of the initial and boundary conditions as well as the mixing processes and thus the changes of the geochemical environment. The impact of the environmental parameters on the distribution coefficients of Cs can be well retraced. A comparison of CPU times needed for the transport simulations employing the conventional K_d-value with those for the new approach using the smart K_d-concept shows only an increase by a factor of 3 – 3.5, which is fully feasible for long-term safety assessment calculations.

CONCLUSIONS

In this work an approach to apply the smart K_d-concept in safety assessment is developed. So-called smart K_d-values are based on mechanistic surface complexation models (SCM) that vary in time and space and depend on the actual geochemical conditions. Therefore, the concept introduced here is based on an appropriate implementation of environmental parameters such as pH, Ca, DIC, ionic strength and radionuclide concentration, which influence the smart K_d-values. Multidimensional smart K_d-matrices for sediments of interest are calculated based on the aforementioned environmental parameters. These calculations are based on thermodynamic sorption models using the component additivity approach. Missing thermodynamic data have been obtained by titration experiments and batch sorption experiments with cesium (Cs^+), strontium (Sr^{2+}), and europium (Eu^{3+}) on orthoclase and muscovite. The feasibility of the component additivity approach has been demonstrated by its application to two different independent sorption experiments.

The whole concept was implemented into the safety assessment transport code r^3t. The results of a 2D test case show that plausible results are achieved and that the method is capable of describing the impact of geochemical changes on sorption of various radionuclides in large model areas over very long time frames. In addition the increase of calculation costs compared to the conventional method using constant K_d-values is low allowing this approach to be used in long-term safety assessments.

REFERENCES

1. NEA: Methods for Safety Assessment of Geological Disposal Facilities for Radioactive Waste. Nuclear Energy Agency (2012).
2. BMU: Sicherheitsanforderungen an die Endlagerung wärmeentwickelnder radioaktiver Abfälle (Safety Requirements for the Final Disposal of Radioactive Waste), Bundesministerium für Umwelt, Naturschutz und Reaktorsicherheit (German Federal Ministry for the Environment, Nature Conservation and Nuclear Safety), Berlin (2010).
3. NAGRA: Project Opalinus Clay: Safety Report. Demonstration of Disposal Feasibility (Entsorgungsnachweis) for Spent Fuel, vitrified High-level Waste and Long-lived Intermediate-level Waste. Nagra Technical Report NTB 02-05. Nagra, Wettingen, Switzerland (2002).
4. POSIVA: Safety Case for the Disposal of Spent Nuclear Fuel at Olkiluoto – Synthesis 2012. Report POSIVA 2012-12 (2012).
5. SKB: Long-term safety for the final repository for spent nuclear fuel at Forsmark. Main report of the SR-Site project. Technical Report TR-11-01, Svensk Kärnbränslehantering AB, (2011).
6. Arnold, T., Zorn, T., Zaenker, H., Bernhard, G., Nitsche, H.: Sorption behavior of U(VI) on phyllite: experiments and modeling. J. Contam. Hydrol. **47**, 219-231 (2001).
7. Davis, J. A., Coston, J. A., Kent, D. B., Fuller, C. C.: Environ. Sci. Technol., **32**, 2820-2828 (1998).
8. Brendler, V., Vahle, A., Arnold, T., Bernhard, G., Fanghänel, T.: RES³T-Rossendorf expert system for surface and sorption thermodynamics, J. Cont. Hydrol., **61** 281-291 (2003).
9. Stockmann, M., Flügge, J., Schikora J., Noseck, U., Brendler, V.: Smart K_d-concept in reactive transport modeling for radioactive waste repositories. To be published.
10. Klinge, H., Köthe, A., Ludwig, R.-R., Zwirner, R.: Geologie und Hydrogeologie des Deckgebirges über dem Salzstock Gorleben, Z. Angew. Geol., **2** 7-15 (2002).
11. Noseck, U., Brendler, V., Flügge, J., Stockmann, M., Britz, S., Lampe, M., Schikora, J., Schneider, A.: Realistic integration of sorption processes in transport codes for long-term safety assessments, Final Report GRS-297, (Gesellschaft für Anlagen- und Reaktorsicherheit (mbH)), Braunschweig 293 p., (2012).
12. Fein, E., Software Package r^3t. Model for Transport and Retention in Porous Media, GRS-192, BMWA-FKZ 02E9148/2, Gesellschaft für Anlagen- und Reaktorsicherheit (GRS) mbH, Braunschweig 319 p. (2004).
13. Parkhurst, D.L., and Appelo, C.A.J., User's guide to PHREEQC (Version 2) - A computer program for speciation, batch-reaction, one-dimensional transport, and inverse geochemical calculations: U.S. Geological Survey Water-Resources Investigations Report, 99-4259, 312 p. (1999).
14. Klinge, H., Boehme, J., Grissemann, C., Houben, G., Ludwig, R.-R., Rübel, A., Schelkes, K., Schildknecht, F., Suckow, A.: Standortbeschreibung Gorleben, Teil 1: Die Hydrogeologie des Deckgebirges des Salzstocks Gorleben, Geol. Jb., **C 71**, 199 p. (2007).
15. Britz, S.: Sorption studies of Eu^{3+} on muscovite and orthoclase. To be published.
16. Poeter, E.P., Hill, M.C., Banta E.R., Mehl, S., Christensen, S.: UCODE_2005 and Six Other Computer Codes for Universal Sensitivity Analysis, Calibration, and Uncertainty Evaluation, U.S Geological Survey, Techniques and Methods 6-A11 299 p (2005).
17. Brasser, T., Scherschel C., Brendler, V., Richter, A., Nebelung, C, Veerhoff, M., Klinger, C., Reichelt,C., ISDA - Ein Integriertes Sorptions-Datenbanksystem. GRS-Report 248, BMBF-02C1144/54/64/74, Gesellschaft für Anlagen- und Reaktorsicherheit (GRS) mbH, Braunschweig (2008).
18. Nebelung, C., Brendler, V., U(VI) sorption on sandstone, IRC Annual Report 2006, Wissenschaftlich-Technische Berichte FZD 456, Dresden, 2007, p. 51.
19. Flügge, J., Radionuclide Transport in the Overburden of a Salt Dome – The Impact of Extreme Climate States, Verlag Dr.Hut, München 209 p (2009).

20. Fein, E., Schneider, A.: d³f – Ein Programmpaket zur Modellierung von Dichteströmungen, GRS-139, BMWi-FKZ 02C04650, Gesellschaft für Anlagen- und Reaktorsicherheit (GRS) mbH, Braunschweig (1999) 245 p.
21. Klinge, H., Baharian-Shiraz, A.: Projekt Gorleben, Dokumentation hydrogeologischer Basisdaten, Hannover (Bundesanstalt für Geowissenschaften und Rohstoffe), 16 (2004).
22. Kitamura, A., Fujiwara, K., Yamamoto, T., Nishikawa, S., Moriyama, H., Analysis of adsoption behavior of cations onto quartz surface by electrical double-layer model, Journal of Nuclear Science and Technology, **36** (12) 1167-1175 p (1999).

ACKNOWLEDGEMENTS

This cooperation project between HZDR and GRS Braunschweig is funded under contract numbers 02 E 10518 and 02 E 10528 as well as 02E 11072A and 02E 11072B by the German Federal Ministry of Economics and Energy on the basis of a decision of the German Bundestag. We would like to thank Michael Lampe (Goethe Center for Scientific Computing (G-CSC), Goethe University Frankfurt) for his work in implementing the smart K_d-concept in the transport code r³t.